J. Fluid Mech. (1968), *vol.* 34, *part* 3, *pp.* 465–480
Printed in Great Britain

Turbulent front structure of an axisymmetric compressible wake

By ANTHONY DEMETRIADES
Philco-Ford Corporation, Newport Beach, California

(Received 30 November 1967 and in revised form 6 May 1968)

Intermittency measurements have been performed within the first 100 virtual diameters of an axisymmetric compressible wake. The primary measurements, performed with the hot-wire anemometer, concerned the intermittency factor and the frequency of 'zero crossings'. The intermittent flow covered most of the wake profile but for a narrow region about the axis, and was found to be normally distributed around the average front position. The latter, along with the extent of the front standard deviation, was found to agree numerically with expectations based on low speed wakes and to grow as the $\frac{1}{3}$ power of axial distance. A weak periodicity of the front was detected at a wavelength about nine times greater than the longitudinal scale of turbulent velocity fluctuations. This periodicity affects the turbulent spectra.

1. Introduction

It is well known that turbulent flows spreading into ambient, quiescent fluid are separated from the latter by a sharp, irregular front or interface. This front changes shape continuously with time, but on the average it advances into the ambient fluid engulfing the latter and making it turbulent. In shear turbulence this motion is accompanied by an over-all movement of the front along the direction of the shearing motion as well. There are at least three practical objectives motivating the study of this front. First, its statistical properties are necessary for the quasi-steady geometrical description of shear zones such as boundary layers, jets and wakes. Secondly, the correct measurement of the net turbulence properties within the front requires the recognition and separation of those effects on the turbulence signal which are due to the intermittent nature of the front itself. Finally, the more detailed the understanding of ambient fluid engulfment and conversion is, the better will be the prediction of the bulk properties of the shear flow, such as thickness and lateral expansion.

This paper deals primarily with the geometrical features of the front and more specifically with the most probable front position, the standard deviation (a measure of the 'wrinkle' amplitude), and the front microscale (a measure of the front wavelength). A considerable investigation of these features has been performed at low speeds with such flows as jets, wakes and boundary layers: compendia of these studies have been presented by Corrsin & Kistler (1953), and more recently by Townsend (1966). These compendia show that the qualitative

features of the front irregularity follow some general rules irrespective of flow geometry; on the other hand, quantitative differences, such as the ratio of the standard deviation σ to the average front position $\overline{Y}$, have been noted among boundary layers, jets and wakes. Furthermore, corresponding front characteristics for the axisymmetric wake have not been reported to date in comparable thoroughness and detail, although some tentative intermittency observations in sphere wakes have been reported by Hwang & Baldwin (1966) and Gibson, Lin & Chen (1967). A curious phenomenon recorded in the course of these studies is the appearance of rather extensive stretches of irrotational flow on the wake axis where fully turbulent flow is usually noted in the results of other experiments of this type.

The dual objective of the present work was to concentrate on an axisymmetric wake and to study this wake at supersonic speeds where compressibility effects are important. High-speed measurements of the front structure are virtually non-existent, with the exception of the statistical interpretation of ballistic-range photographs of wakes carried out to some detail by Schapker (1966) and Levensteins & Krumins (1967). This optical method has revealed certain important similarities between low- and high-speed front behaviour as regards, for example, the distribution of intermittency factor and the variation of the front microscale with distance. Unfortunately, and in addition to observational difficulties, the intermittent properties so found can only be related to gross flight parameters (e.g. body shape and size) rather than the more meaningful integral wake properties (e.g. the drag, transverse scale, etc.) obtainable by a complete mapping of the flow field such as is possible in wind tunnels. The latter prerequisite has already been fulfilled in the present case, since complete mean and turbulent flow measurements of the axisymmetric wake at hand were already available. Using this well-probed wake flow, additional measurements were made including the intermittency factor recorded with a special electronic circuit, the frequency of 'zero-occurrences' and spectral measurements of the fluctuations. Sufficient information was thus gathered to deduce: (i) the position of the turbulent front, (ii) the front standard deviation, and (iii) the average wavelength of the front.

2. Wake flow field

An axisymmetric turbulent wake was produced at a stream Mach number 3 and a Reynolds number of 50,000/cm by cantilevering a 0·396 cm diameter rod through the throat of the Philco–Ford supersonic continuous wind tunnel. The rod ended slightly beyond the upstream apex of the uniform-flow rhombus into which it shed a turbulent wake of (momentum) diameter 0·216 cm. Ordinary instrumentation was employed to map in detail the distribution of mean and fluctuating values of the flow properties such as the velocity and the temperature, for a distance extending to about 90 diameters beyond the model base. Besides furnishing local velocities useful in the reduction and interpretation of intermittency data, these maps made possible the computation of scale lengths, whether mean or turbulent, useful for comparison with intermittent scale lengths.

It is hardly surprising that beyond a relaxation distance of about 40 diameters the wake decelerates with respect to the surrounding flow to the point where its radial property profiles correlate into a Gaussian distribution and where its axial variations follow closely low-speed decay laws: the velocity defect

$$w \equiv (u_\infty - u(0))/u_\infty$$

and temperature defect $\theta = (T(0) - T_\infty)/T_\infty$ decrease as the inverse $\frac{2}{3}$ power of distance, and the transverse scale L (equal to the l_0 defined by Townsend (1956)) increases as the $\frac{1}{3}$ power of distance. The wake Reynolds number based, as usual, on L and $(u_\infty - u(0))$ thus decreases from an initial 1500 to about 500, while the Reynolds number based on the turbulence velocity and the macroscale size lay between about 200 and 1000.

3. Instrumentation and procedure

Intermittency measurements require a tool capable of recording the time the hot-wire is immersed in the turbulent flow versus the time it is not. Perhaps the most direct method is to perform the statistics *in situ* by means of an electronic circuit such as used, for example, by Corrsin & Kistler (1953) and Bradbury (1965). An intermittency circuit for measuring the intermittency factor directly from a hot-wire anemometer signal was constructed by modifying the latter authors' circuitry for higher frequency response. The instrument utilized seven operational amplifiers and associated feed-back networks for signal processing. A signal level of up to 10 volts peak-to-peak could be handled effectively by this system making it compatible with the constant-current hot-wire anemometer amplifier employed. All amplifiers used in the system to process the a.c. signal were 100 volts/μsec slewing rate providing an extremely fast response instrument for measuring the intermittency. The circuit also provided a 0- to 1-volt d.c. output directly proportional to the intermittency factor, which could thus be read directly on the face of a panel meter or used to drive a d.c. recorder. It was initially hoped that the wire could be traversed continuously through the wake, and the d.c. output noted directly on the recorder. As other investigators also found, however, the trigger level and other circuit controls required adjustment from point to point, so that the intermittency measurement was not quite that simple. At each point many dual-trace oscillograms of the wire output and the rectangular-pulse trigger output were thus obtained; the trigger level was then varied and the intermittency factor was recorded only when the rectangular pulse rose at the exact beginning of the turbulence 'burst' and fell at its exact end. For these measurements, a calibrated 0·00005 in. diameter platinum 10% rhodium wire was used. Its current was first adjusted to the maximum safe value so that no melting would occur anywhere across the wake; the amplifier was also adjusted to overcome thermal lag effects on the frequency response. The wire was then lowered at a point in the wake and, after suitable adjustment of the circuit controls, the intermittency factor γ was noted. This process was repeated at each of about 22 radial positions and at each of the 14 axial positions along the wake. At each point the signal was first observed on a Tektronix type

549 storage oscilloscope for the purpose of making the required adjustments in signal amplification and especially in the trigger level. The trace storage technique, a new development in oscillography, proved an invaluable aid in recording γ correctly. By freezing the trace on the scope screen for an arbitrary controllable period (from a fraction of a second to one hour) the operator can determine much better than hitherto possible whether the Schmidt circuit triggers properly. The factor γ was given by the circuit meter directly as the fraction of one volt d.c. (e.g. 0·68 volt denotes $\gamma = 0{\cdot}68$).

A similar procedure was followed in measuring the frequency N of zero occurrences, i.e. the number of times per second the wire crosses the front. The rectangular-pulse shape of the trigger output afforded a relatively simple way by which this frequency could be measured. This was done by directing the trigger output signal into a counter whose own trigger level was set below 1 volt d.c. The crossing frequency (also called the frequency of zeros) was then read directly by the counter. This measurement was also made at each of the 14 axial positions noted above although at a fewer radial positions for each. Reading the zero frequencies required, of course, the same adjustments of the intermittency circuit and amplifier as during the measurement of γ.

A third series of measurements consisted of a spectral and modal analysis of the hot-wire output at different positions inside the turbulent wake. This yielded the one-dimensional (longitudinal) spectra of temperature and axial velocity fluctuations which supplied, in the low-frequency limit, the necessary data for the computation of the relevant integral scales. Spectra were also obtained of the Schmidt-trigger output of the intermittency circuit. This signal has the familiar form of rectangular waves of constant artificial amplitude but varying spacing and duration and, ideally speaking, represents the temporal behaviour of the turbulent front viewed as a stationary variable random in time

4. Results

Figure 1 shows the distribution with radius of the intermittency factor γ at each of the 14 axial positions examined; here $\eta = Y/L$, where Y is the Howarth–Dorodnitsyn radius:

$$Y^2 \equiv 2\int_0^y \frac{\rho}{\rho_\infty} y\,dy,$$

with ρ the local density and ρ_∞ the density outside the wake, and where L is the transverse wake scale defined further below. Nearer the body the region of fully turbulent fluid ($\gamma = 1$) is noticeably broader around the axis, but further downstream γ departs from unity almost immediately off the axis. It appears, therefore, that in the self-preserving region (beyond $\bar{x} = 40$) the fully turbulent fluid is confined to the very immediate vicinity of the wake axis; this is in general agreement with the two-dimensional wake at low speeds (Townsend 1956). The occurrence, if any, of laminar spots on the axis of this wake is highly improbable, in noteworthy contrast to the extent to which such spots appeared in the sphere wakes of Gibson *et al.* (1967) and Hwang & Baldwin (1966). In fact, a separate experiment was performed wherein 154 oscillograms of the turbulence on the

axis were obtained, of which not one showed evidence of laminar (external) flow. Each of these was of 200 μs duration which, at a wake thickness of order 1 cm and a stream speed of about 60,000 cm/s, confirms conclusively the high improbability of $\gamma < 1$ on the axis. Figure 2 shows a comparison, at a typical axial position $\bar{x}$, of the distribution in γ and in the velocity $\tilde{u}$ and temperature $\tilde{T}$,

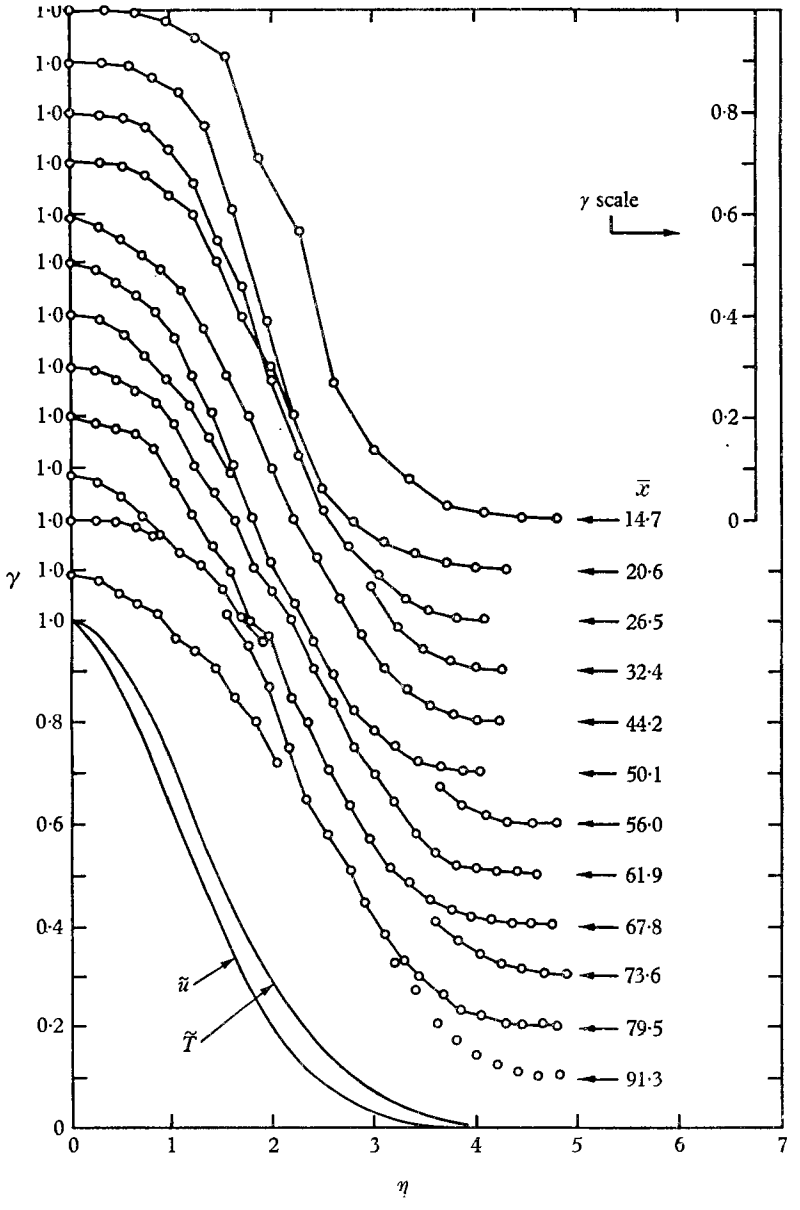

FIGURE 1. Distribution of the intermittency factor γ with non-dimensional radius $\eta = Y/L$ for various axial distances $\bar{x} \equiv (x-x_0)/(C_D A)^{\frac{1}{2}}$. Similarity profiles of non-dimensional velocity $\tilde{u} \equiv (u_\infty - u)/(u_\infty - u(0))$ and temperature $\tilde{T} \equiv (T-T_\infty)/(T(0)-T_\infty)$ are shown for comparison.

where $\tilde{T} \equiv (T - T_\infty)/(T(0) - T_\infty)$ and $\tilde{u} \equiv (u_\infty - u)/(u_\infty - u(0))$. It is significant that turbulent bursts appear at the edges of the wake (especially at high $\bar{x}$) where the sensible axial wake motion has all but vanished; for example, at $\eta = 3{\cdot}28$, $\tilde{u} = 0{\cdot}01$ while $\gamma = 0{\cdot}17$.

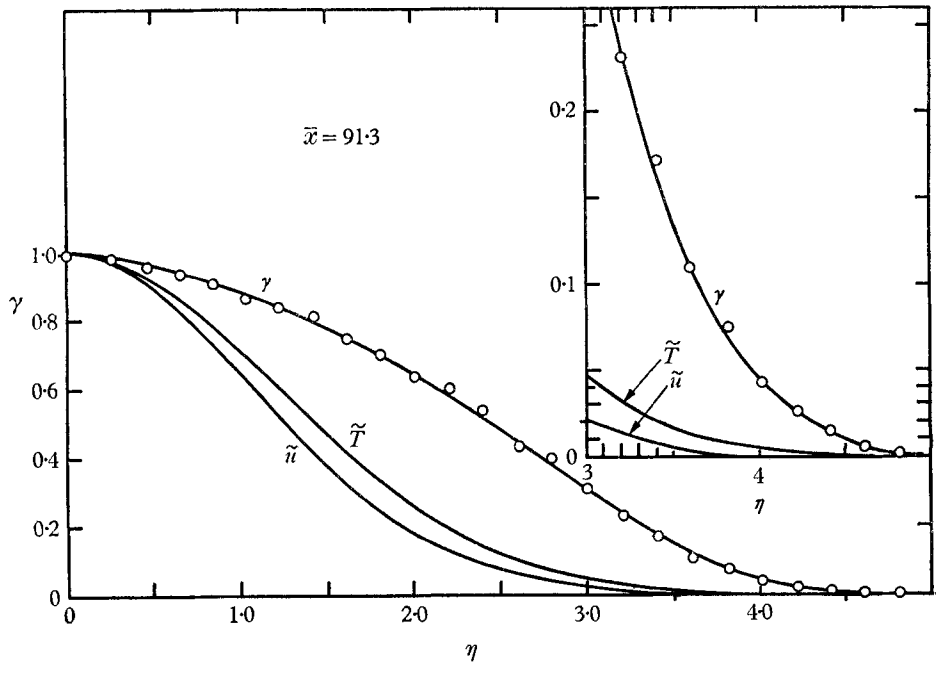

FIGURE 2. Comparison of intermittency factor, temperature and axial velocity variation at $\bar{x} = 91{\cdot}3$.

The data of figure 1 were used to compute the mean position $\overline{Y}$ of the turbulent front and its standard deviation σ defined† by

$$\overline{Y} = \int_0^\infty Y \frac{d\gamma}{dY} dY$$

and

$$\sigma \equiv \left[\int_0^\infty (Y - \overline{Y})^2 \frac{d\gamma}{dY} d(Y - \overline{Y})\right]^{\frac{1}{2}}.$$

In order to perform these computations the distributions of figure 1 were curve-fitted by polynomials of the form

$$\gamma = \sum_n A_n Y^n$$

with the aid of the Philco 2000 digital computer. Adequate fits were obtained for 6th to 8th order polynomials, the aim being to minimize the computed standard deviation between the polynomial and the experimental curve. The results of

† A thorough discussion of the processing and interpretation of intermittency measurements, togther with the necessary background from the theory of stationary random variables, has been given by Corrsin & Kistler (1953).

this computation are shown on figure 3. The transverse scale L used here to non-dimensionalize the data was found, as noted earlier, to follow closely the low-speed self-preserving behaviour over most of the wake:

$$L \equiv \left[\frac{C_D A}{4\pi} \frac{u_\infty}{u_\infty - u(0)}\right]^{\frac{1}{2}},$$

where u_∞ and $u(0)$ are the velocity outside the wake and on its axis, respectively. When the numerical dependence of $u(0)$ on the properly normalized axial distance

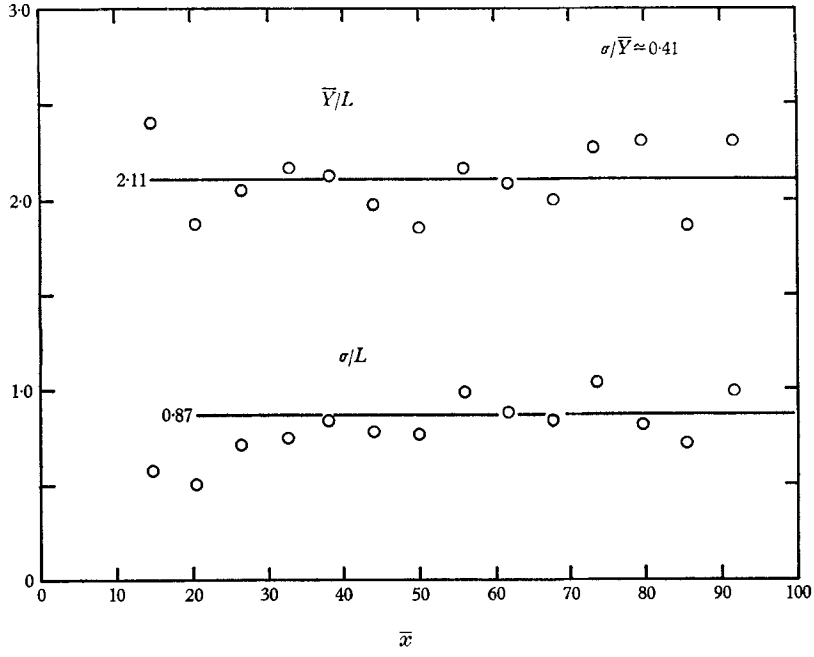

FIGURE 3. Comparison of the average front position $\overline{Y}$, standard front deviation σ and transverse wake scale L.

$\bar{x} = (x - x_0)/(C_D A)^{\frac{1}{2}}$ is substituted in the above equation, one obtains for the present experiment:

$$L = 0{\cdot}264(C_D A)^{\frac{1}{2}} \bar{x}^{\frac{1}{2}},$$

where $(C_D A)^{\frac{1}{2}} = 0{\cdot}216$ cm. The average of the points shown gives $\overline{Y} = 2{\cdot}1L$ and $\sigma = 0{\cdot}87L$. The front is thus located at a point two-thirds times the distance between the axis and the wake 'edge' $\eta(\tilde{u} = 0{\cdot}01) = 3{\cdot}28$. A test of the skewness in the distribution of the probability $d\gamma/dY$ was made by comparing the radial position of the maximum values of $d\gamma/dY$ with the $\overline{Y}$ as found above. These two agreed within 4 % of each other, confirming that the skewness was indeed minimal.

Using the computed value of σ it is possible to plot the distribution of the factor γ about the front position $\overline{Y}$, as shown on figure 4. With the exception of the two axial positions closest to the body, all data points fall on a well-defined curve which is in fact identical to that encountered for most other free turbulent flows. The distribution shown is hardly surprising on statistical ground, but it is still

interesting since it involves flows of widely varied types, flow speeds and methods of diagnosis.

Figure 5 shows the distribution of the frequency N of zeros with axial and radial distance. As expected, the frequency is zero on the axis and outside the wake and it peaks near the turbulent front. The distribution of the zeros N about the mean is quite symmetric and the shift of the $Y_{\max}$ ($N_{\max}$) with $\bar{x}$ is quite clear. The peak

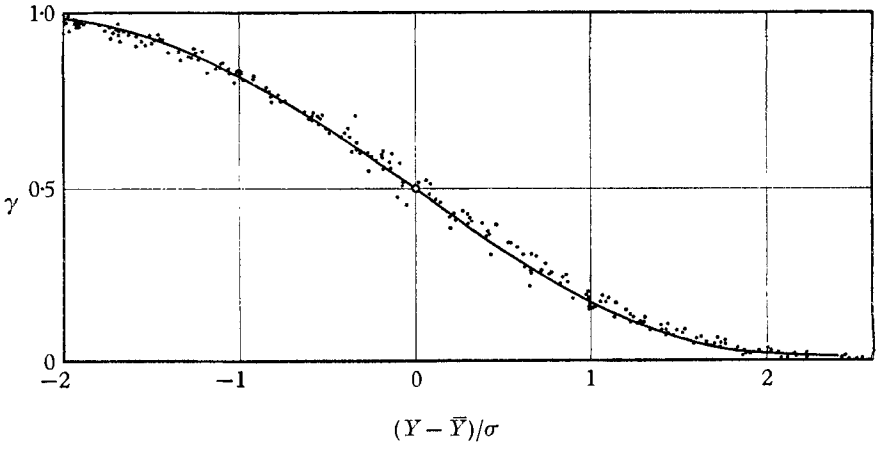

FIGURE 4. Distribution of intermittency factor about the front position. Solid line averages previous results from a circular jet (Corrsin & Kistler 1953) a hot-wire study of a two-dimensional wake at low speed (Townsend 1956) and a photographic study of a hypervelocity projectile (Levensteins & Krumins 1967).

frequency, originally lying at about 20 kc/s gradually shifts to about 30 kc/s far downstream. The $N_{\max}$ and $Y_{\max}$ were found by curve-fitting the data of figure 5 with polynomials of the type

$$N = \sum_n B_n Y^n.$$

Further, the symmetry of the zero occurrences was then checked by plotting the normalized zero frequency $N/N_{\max}$ about $Y/Y_{\max}$. The symmetry of these results, shown in figure 6, is gratifying and the resemblance to a Gaussian distribution is quite close. Finally, because both the intermittency factor γ and the zeros N are distributed in a normal (Gaussian) fashion as shown by the preceding figures, it is possible to evaluate the autocorrelation microscale λ_F of the turbulent front by:

$$\lambda_F = \frac{\sqrt{2}}{\pi} \frac{u(\overline{Y})}{N_0}.$$

In this connexion it is relevant to ask whether the scale $\Lambda_F = u(\overline{Y})/N_0$ itself does not have a physical significance, especially because of the repeatability observed in measuring N_0. Since N_0 is the 'average number of zeros' Λ_F must have the meaning of an 'average wavelength' which is, of course, $\pi/\sqrt{2}$ times larger than λ_F. Almost exactly the same numerical difference between Λ_F and λ_F was also observed by Corrsin & Kistler who computed Λ_F from measurements of the average extent of the laminar and non-laminar regions at $Y = \overline{Y}$. This disparity

was of seemingly minor importance in the latter instance because no phenomena were observed to give Λ_F a physical foundation.

In the present case additional phenomena featuring a wavelength Λ_F were observed in the course of making spectral measurements in the turbulent wake.

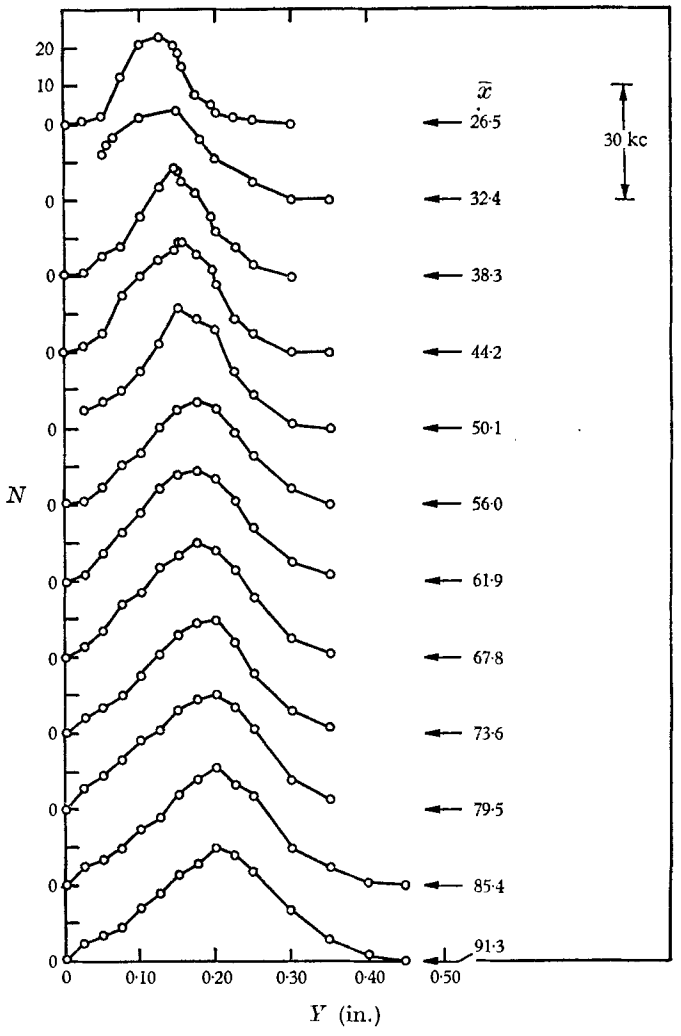

FIGURE 5. Distribution of the frequency of zero occurrences N with wake radius for various axial distances.

Figure 7 shows one-dimensional spectra of the density (temperature) and velocity fluctuations taken at various positions along the radius at a fixed axial position. A concentration of fluctuation energy appears at a frequency f_T in the vicinity of 30 kc/s. A test was performed in which these spectra were further compared with the output spectrum of the trigger network of the intermittency circuit. From this test, which is shown on figure 8, there is little doubt that the 'peak' remains in the spectrum even when the bona fide turbulence is by this

means suppressed. This peak, in other words, is due to the 'clipped' signal constituted by the intermittency, rather than the turbulence, output of the hot-wire. It is therefore reasonable to suppose that the phenomena of frequency N_0 in the zero-occurrence measurement as well as those of frequency f_T in the spectral measurements arise from the same source, i.e. an organization of the front into a periodic structure. Figure 9 plots the two wavelengths

$$\Lambda_F \equiv u(\overline{Y})/N_0 = u(\overline{Y})/f_T,$$

which are seen to be about equal farther along the wake; this equality could anyway be predicted earlier since N_0 and f_T were found to be about equal. No explanation exists for the differences below $\bar{x} = 50$, however. A value $\Lambda_F/L = 9 \pm 2$ seems to prevail. It will be recalled from previous remarks that this wavelength is thus about twice the statistical wake diameter $2\overline{Y}$, i.e. $\Lambda_F \simeq 4\overline{Y}$.

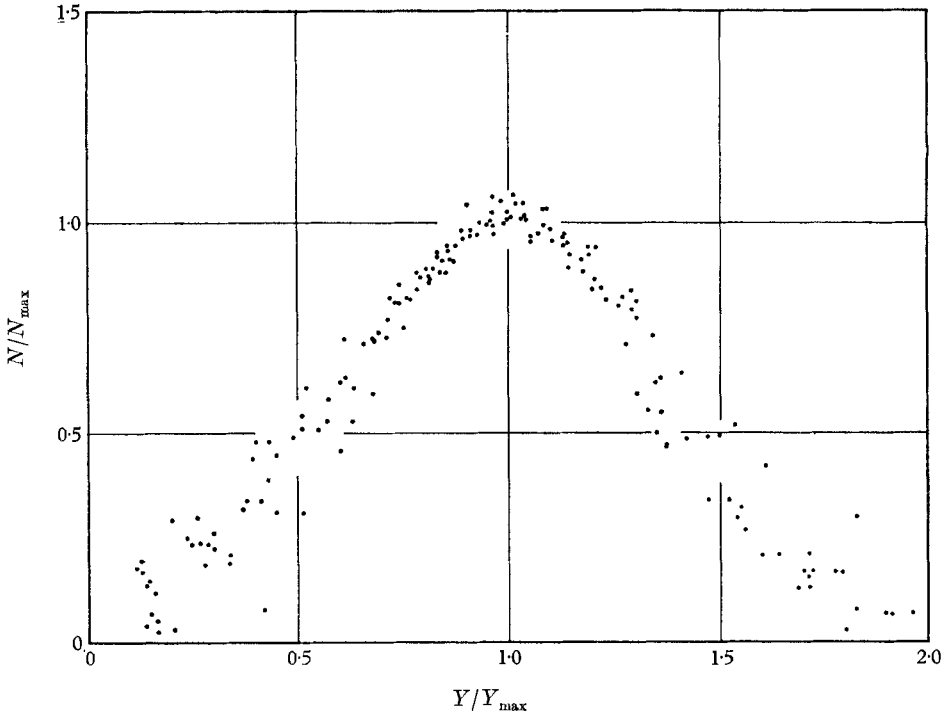

FIGURE 6. Normalized distribution of zero occurrences. Y_{max} corresponds very closely to the front position $\overline{Y}$.

5. Discussion

5.1. *Wavelength of turbulent front*

The generally accepted view of the shape of the turbulent front is that it is random about its mean position, as sketched in figure 10 (*a*). The Schmidt trigger output spectra obtained by Corrsin & Kistler (1953) had the characteristic 'Poisson' shape supporting this view. In the present instance we may, for purposes of illustration, advance the possibility that a structure of more primitive form, such as in figure 10 (*b*), is involved. We must admit that in reality one

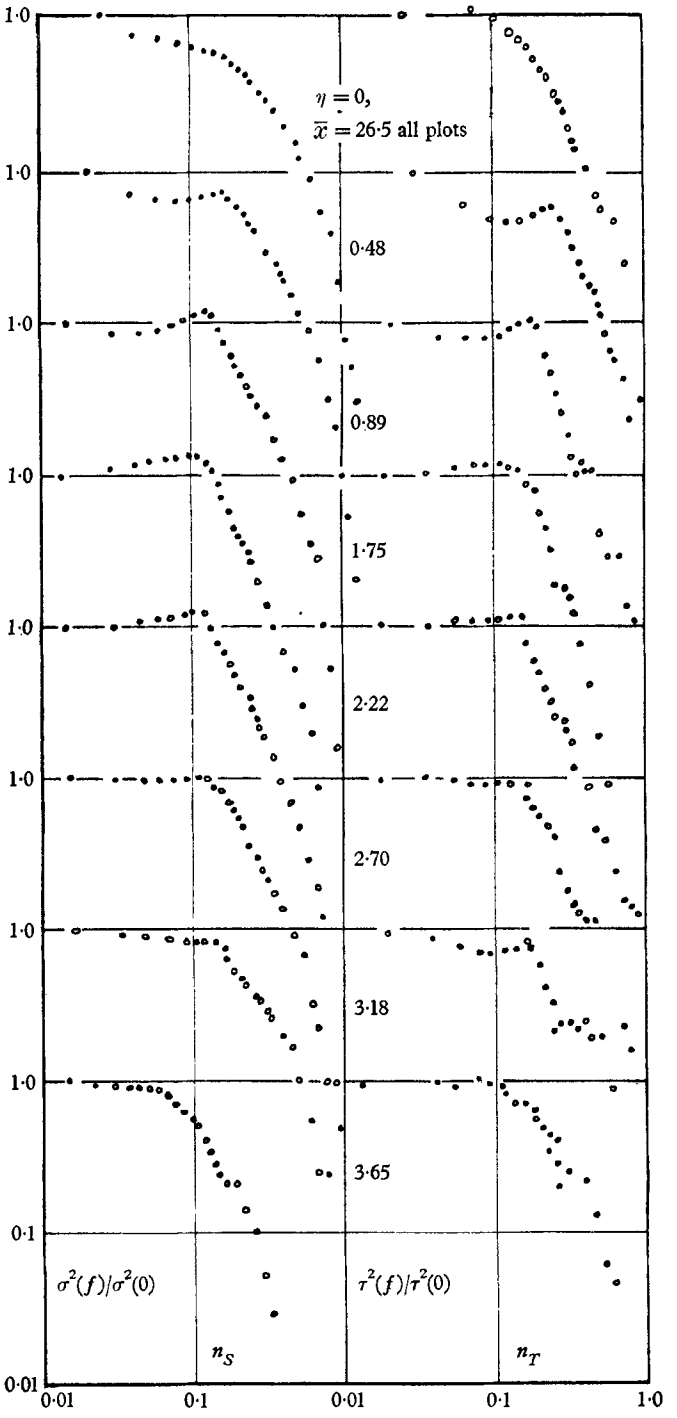

FIGURE 7. Normalized longitudinal spectra of density $\sigma^2(f)/\sigma^2(0)$ and axial velocity $t^2(f)/t^2(0)$ at $\bar{x} = 26{\cdot}5$ and at various radial positions. Frequencies are nondimensionalized with integral scales Λ and local velocity u: $n_s \equiv f\Lambda_s/u$, $n_T \equiv f\Lambda_T/u$.

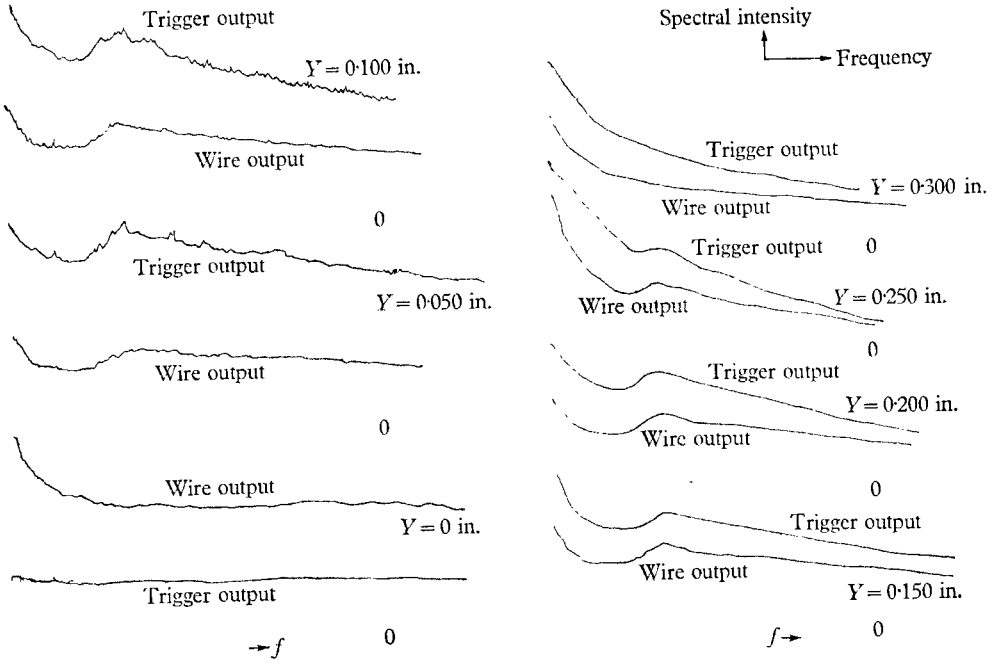

FIGURE 8. Comparison of turbulence and trigger output spectra at fixed $\bar{x}$ and at various radial positions Y.

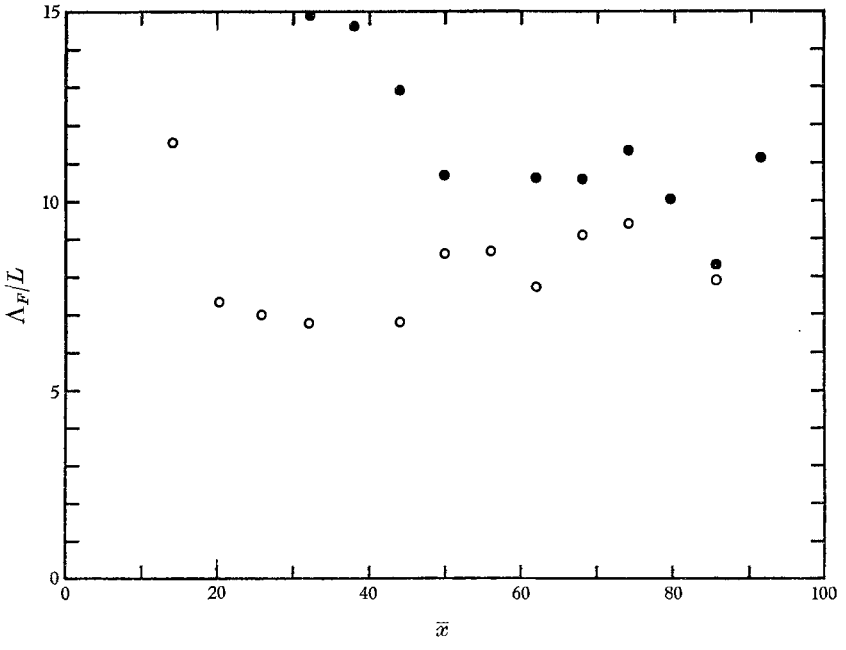

FIGURE 9. Variation of front wavelength Λ_F with axial distance. $\Lambda_F/L = u(\bar{Y})/LN_0$. ○, N_0 from spectra; ●, N_0 from zero occurrences.

obtains a mixture of both phenomena, and in fact the Schmidt trigger output spectrum of figure 8 looks much like the 'Poisson' spectrum but with a peak superimposed. We can conclude that the periodic structure is indeed tenuous, perhaps appearing and disappearing cyclically as suggested by Townsend (1966) and Grant (1958). The former of these authors has recently (Townsend 1966) made calculations of possible front indentations based on stability arguments and finds that such waves may have a wavelength between $6L$ and $7L$.

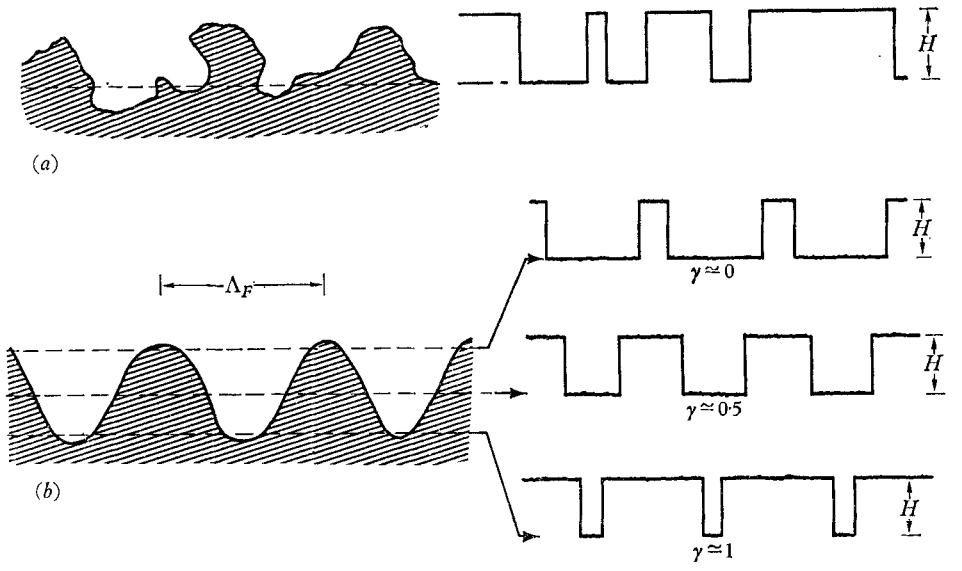

FIGURE 10. Typical response of trigger circuit for (*a*) a 'real' front configuration and (*b*) an 'ideal' front configuration.

The ability to further these first impressions of the front periodicity hinges on the success of separating the real turbulence from the intermittency in the hot-wire anemometer output. In the meantime, useful guidelines can be drawn from the elementary suggestions of figure 10(*b*). In the unlikely case where H is constant, for example, the periodicity will never evidence itself at a single frequency, since the wave shape of the wire output f is given by

$$f(t) = \gamma H + \frac{2H}{\pi} \sum_{1}^{\infty} \frac{\sin n\pi\gamma}{n} \left[\cos n\omega t \cos \frac{n\pi\gamma}{2} - \sin n\omega t \sin \frac{n\pi\gamma}{2} \right],$$

whose spectrum is discrete, with the component n having a mean-square value $2H^2 \sin^2 n\pi\gamma / \pi^2 n^2$. Further, the mean-square fluctuation $\overline{(\Delta f)^2}$ of f varies as $H^2\gamma(1-\gamma)$ which peaks at $\gamma = 0{\cdot}5$, i.e. at the front position $\overline{Y}$. This is indeed well substantiated by the spectra of figure 7, showing that the peak attains a maximum in the region between $\eta = 1$ and $\eta = 2{\cdot}5$ and vanishes at the extremities where $\gamma = 0$ and $\gamma = 1$.

5.2. *Comparison with other experiments*

In low-speed flows, Corrsin & Kistler (1953) have observed that γ is distributed with $(Y-\overline{Y})/\sigma$ in a manner independent of the type of flow (wake, jet or boundary layer); this 'universal' curve agrees well with the present results, as already shown on figure 4. This agreement is, of course, fully expected since γ, σ and $\overline{Y}$ are in essence moments of each other. It is hardly surprising, therefore, that measurements subject to added natural aberrations, such as the ballistic-range measurements of Levensteins & Krumins (1967) show equally good agreement. It is much more significant to relate the intermittency behaviour to the transport of momentum across the turbulent flow. Thus, the spreading rates of $\overline{Y}$ and σ, as Corrsin demonstrated, follow the dependence of the flow scale L on distance $\bar{x}$ and are thus dependent on the type of flow at hand. It has already been seen that in the present wake $L \sim \bar{x}^{\frac{1}{3}}$, and in figure 3 of this paper the relationship $\sigma \sim \overline{Y} \sim L \sim \bar{x}^{\frac{1}{3}}$ is fully verified; in Townsend's cylinder wake $\sigma \sim \overline{Y} \sim L \sim \bar{x}^{\frac{1}{2}}$ as expected.

	Present work (wake)	Townsend (1956) (wake)	Grant (1958) (wake)	Bradbury (1965) (jet)
$\overline{Y}/L$	2·1	2·1	2·1	2·0
σ/L	0·87	0·80	0·80	0·44
$\sigma/\overline{Y}$	0·41	0·38	0·38	0·22
$\Lambda_u/\overline{Y}$	0·5	0·5	0·5	0·55
Λ_u/L	1	1·06	1·06	0·92*
Λ_u/Λ_T	0·5 – 1†	—	—	0·58*
λ_F/L	4·6	—	—	—
Λ_F/L	9 ± 2	—	—	—
$\eta(\bar{u} = 0{\cdot}01)/L$	3·28	—	—	—
$\eta(\gamma = 0{\cdot}01)/L$	4·5	—	—	—

* Data from Corrsin & Uberoi (1950).
† 0·5 on wake axis, 1·0 near wake edge.

TABLE 1. Characteristic lengths of wake compared with low-speed experimental results.

Table 1 shows a numerical comparison of the present results with those available from low-speed experiments. It should be noted that the position $\overline{Y}$ of the front and the turbulent macroscales Λ_u (the longitudinal velocity scale) and Λ_T (the longitudinal temperature scale) seem to be constant for different types of flow; the standard deviation differs for the jet and, as Townsend (1966) points out, for the boundary layer as well. This difference has been attributed by Gartshore (1966) to differences in the effective turbulence Reynolds number R_T among such flows. His exact expression, put into the present nomenclature reads

$$\frac{\sigma}{L} = \frac{2{\cdot}97}{\sqrt{R_T}},$$

which gives $\sigma/L = 0{\cdot}83$ for the $R_T = 12{\cdot}8$ found in the present experiment. Note that a slight difference between the above equation and Gartshore's formula

exists because the transverse scale L is about 22 % smaller than Gartshore's L_0 which is the flow 'half radius'.

As previously noted, no stretches of ambient (irrotational) fluid were found on the wake axis. This is in contrast with the results of Gibson *et al.* (1967) and Hwang & Baldwin (1966) and a tentative explanation of the difference can be given by combining Gartshore's results with a brief critique made by Behrens (1963) of low-speed wake experiments, notably those of Reichardt & Ermshaus (1962). Behrens observed that the turbulent Reynolds number R_T for axisymmetric bodies is not constant but varies with bluntness, from about 1 for very blunt (say, disks normal to the flow) to about 10 for very slender bodies; at the latter extreme R_T is about equal to that for two-dimensional wakes (in the present wake $R_T = 12{\cdot}8$ was obtained, very close to the value of 12·7 for cylinders at low speeds). Further along the scale one can obtain R_T as high as 30, 40 or 50 for jets. Gartshore's formula predicts that large differences in the standard deviation σ should therefore result from such large differences in R_T. Therefore, in the present experiment ($R_T = 12{\cdot}8$) σ has increased to the point where the axis barely escapes an occasional brush with the external flow, but for blunt axisymmetric bodies the 'wrinkle amplitude' represented by σ should become so large (it is $\sigma/L \simeq 3$ at $R_T = 1$; in the present work we have $\sigma/L = 0{\cdot}87$) that the front corrugation depth reaches and exceeds the wake axis. In the latter case the wake would no longer resemble a straight cylinder with rough surface but rather a cylinder with grossly ondulating axis. It is very likely that the wakes examined by Gibson *et al.* and Hwang & Baldwin belong in this latter category.

6. Conclusions

We draw the following conclusions from the experiment described above.

A fully turbulent region exists about the axis of the wake; this region is very narrow in extent (compared to the wake diameter) in the self-preserving region. No occurrence of irrotational flow on the axis, of the type observed by Hwang & Baldwin and Gibson *et al.*, was seen.

The wake front $\overline{Y}$ is located at $\eta = 2{\cdot}1$; thus the wake 'diameter' $2\overline{Y}$ is about $4{\cdot}2L$, where L is the transverse scale. The standard deviation of the front corrugations $\sigma = 0{\cdot}87L$. These results are in very good agreement with low-speed experimental results on wakes.

The distribution of γ about the front position (i.e. with $(Y - \overline{Y})/\sigma$) is Gaussian in character and identical with all similar variations reported so far, apparently including ballistic range (hypervelocity) experiments.

The intermittency 'radius' of the wake is located at $\eta(\gamma = 0{\cdot}01) \simeq 4{\cdot}5$, contrasted with $\eta(\tilde{T} = 0{\cdot}01) = 3{\cdot}65$ and $\eta(\tilde{u} = 0{\cdot}01) = 3{\cdot}28$, the 'temperature' and 'velocity' radius respectively.

A weak periodicity in the front geometry was noted with a wavelength $\Lambda_F = 9L \pm 2L$. In the spectral sense this periodicity affects the spectra of turbulence within the wake itself.

REFERENCES

BEHRENS, W. 1963 *GALCIT Hypersonic Project IM-15, Calif. Inst. of Techn., Pasadena, Calif.*

BRADBURY, L. J. S. 1965 *Aero. Quart.* **15**, 281.

CORRSIN, S. & KISTLER, A. L. 1953 *NACA TR* 1244, Washington, D.C.

CORRSIN, S. & UBEROI M. S. 1950 *NACA TR* 998, Washington, D.C.

GARTSHORE, I. S. 1966 *J. Fluid Mech.* **24**, 89.

GIBSON, C. H., LIN, S. C. & CHEN, C. C. 1967 *AIAA Paper*, no. 67–20. New York, N.Y.

GRANT, H. L. 1958 *J. Fluid Mech.* **4**, 149.

HWANG, N. H. C. & BALDWIN, L. V. 1966 *Trans. Am. Soc. Mech. Engr. Ser. D, J. Basic Engr.* **88**, 261.

LEVENSTEINS, Z. L. & KRUMINS, M. V. 1967 *AIAA J.* **5**, 1596.

REICHARDT, H. & ERMSHAUS, R. 1962 *Int. J. Heat Mass Tr.* **5**, 251.

SCHAPKER, R. L. 1966 *AIAA J.* **4**, 1979.

TOWNSEND, A. A. 1956 *The Structure of Turbulent Shear Flow.* Cambridge University Press.

TOWNSEND, A. A. 1966 *J. Fluid Mech.* **26**, 689.